

High resolution cardiac T1 mapping using an adaptive data acquisition algorithm combining navigator gating and compressed sensing

Bhairav Bipin Mehta¹, Xiao Chen¹, Christopher M. Kramer^{2,3}, Michael Salerno^{1,2}, and Frederick H. Epstein^{1,3}

¹Department of Biomedical Engineering, University of Virginia, Charlottesville, VA, United States, ²Department of Medicine, Cardiology Division University of Virginia, Charlottesville, VA, United States, ³Department of Radiology, University of Virginia, Charlottesville, VA, United States

Introduction: MOLLI¹, a preferred clinical myocardial T1 mapping technique, has limited spatial resolution because data are acquired within a breathhold. Higher spatial resolution may improve assessment of thin structures such as the right ventricular and left atrial walls, and the peri-infarct zone. We previously developed an Accelerated and Navigator-Gated look-locker Imaging sequence for cardiac T1 Estimation (ANGIE²), which enables high-resolution T1 mapping by removing the breathhold constraint. ANGIE uses navigator rejection of data acquired outside the respiratory acceptance window, resulting in k_y -t undersampling, and compressed sensing (CS) to reconstruct the undersampled data. For high-quality CS reconstruction, the k_y -t sampling pattern should be incoherent, and to minimize scan time, a stopping criterion to halt acquisition should be based on the capability to perform accurate reconstruction and precise T1 estimation. Typically for CS, the sampling pattern and the acceleration factor are prescribed prior to scanning. However, for navigator methods, decisions regarding rejection of data occur during the scan, and sampling patterns and acceleration factors determined *a priori* are disrupted. We developed an ANGIE sequence that adapts to navigator rejection of data by recalculating, in real-time, a sampling pattern that is well-suited for CS³, and halting data acquisition when k_y -t sampling is sufficient for accurate CS reconstruction and precise T1 estimation. We tested adaptive ANGIE in normal volunteers and compared different adaptive sampling methods by performing retrospective analysis of fully-sampled ANGIE data.

Methods: We implemented adaptive ANGIE on a 1.5T Avanto system (Siemens Healthcare, Erlangen, Germany). The implemented version computed the next k_y -t lines to acquire depending on the current k_y -t sampling pattern and its transform sidelobe-to-peak-ratio (TSPR)⁴, a metric that measures the severity of artifacts due to undersampling. We also used the evolving Cramer-Rao lower bound (CRLB) to measure how precisely T1 could be estimated given the sampled inversion times (TIs)⁵. Data acquisition was halted when the TSPR and CRLB both reached threshold values. CS reconstruction using matrix rank sparsity⁶ was implemented in MATLAB. To compare adaptive ANGIE to MOLLI, we performed acquisitions using standard MOLLI, ANGIE with resolution similar to MOLLI (resolution=1.3-2.1mm²), and high resolution ANGIE (resolution=0.9-1.4mm²) in 5 healthy volunteers (age 24 ± 2 yrs).

Additionally, we compared the reconstruction quality of different adaptive data sampling methods. Specifically, we compared adaptive data sampling based on the TSPR and adaptive data sampling based on a probability distribution function (PDF), using a fully-sampled ANGIE data set that was retrospectively under-sampled (n=9). Undersampling was performed by assuming the same navigator acceptance pattern for the schemes (nonadaptive, TSPR-based adaptive, and PDF-based adaptive) so that the same total number of phase encodes were acquired for each. The particular phase encoding lines differed between schemes as follows. For nonadaptive acquisitions, random phase encode lines determined *a priori* were chosen. For TSPR-based adaptive acquisitions, the phase encode lines that minimized the TSPR of the new k_y -t sampling pattern were chosen. For PDF-based adaptive acquisitions, the phase encode lines that made the phase encode distribution along the k_y direction most uniform, independent of its inversion time, were chosen.

Results Fig. 1 shows an example high resolution T1 map of the heart from a human subject acquired using adaptive ANGIE. The mean scan time for high-resolution adaptive ANGIE for 5 volunteers was 68±18s per slice. Use of an adaptive acquisition reduced ANGIE's scan time by 42% compared to a nonadaptive acquisition. Table 1 compares MOLLI to nonadaptive and adaptive ANGIE. Myocardial T1 estimates are in good agreement among all the acquisitions. Fig. 2 illustrates reduced image artifacts using PDF-based adaptive sampling compared to the nonadaptive and TSPR-based adaptive acquisitions. Table 2 provides a quantitative comparison of the three sampling schemes. Mean squared error and structural similarity index for the PDF-based adaptive sampling were significantly (p<0.05) better compared to other sampling schemes.

Discussion: Adaptive ANGIE accounts for the interplay between navigator rejection of the data and k_y -t sampling patterns that are well-suited for reconstruction by CS, minimizing scan time while maintaining high quality CS reconstruction. As a result, adaptive ANGIE facilitates high-resolution T1-mapping within a clinically acceptable scan time. A PDF-based adaptive acquisition improved CS reconstruction. Adaptive ANGIE is a promising technique for T1 mapping of small structures.

References: (1) Messroghli et al: MRM 2004. (2) Mehta et al: JCMR 2012. (3) Barral et al: Proc. of ISMRM 2009. (4) Lustig et al: MRM 2007. (5) Zhang et al: JMRI 1998. (6) Lingala et al: IEEE TMI 2011.

Acknowledgements: This work was funded by Siemens Medical Solutions and NIH NIBIB R01 EB 001763.

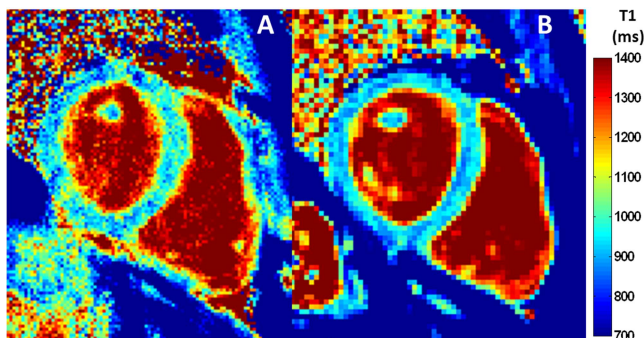


Fig. 1. Example T1 maps acquired from a healthy volunteer. **A:** T1 map using adaptive ANGIE (1.4x1.4 mm²), and **B:** T1 map using MOLLI (2.3x2.8 mm²). ANGIE T1 estimates are in good agreement with MOLLI

Table 2. Quantitative analysis of acquisition algorithms

* p<0.05 for adaptive PDF vs both nonadaptive and adaptive TSPR.

	Nonadaptive	Adaptive TSPR	Adaptive PDF
Mean squared error (10 ⁻¹⁴)	1.007±0.093	1.178±0.180	0.962±0.072*
Structural similarity index	0.7634±0.0190	0.7471±0.0256	0.7694±0.0166*

Table 1. Scan time and myocardial T1 estimate results from healthy volunteers.

	MOLLI	Adaptive ANGIE (high res)	Adaptive ANGIE (low res)	Nonadaptive ANGIE ² (low res)
Scan Time	17 (hb)	68±18 s	47 ± 13 s	81 ± 28 s
Myocardial T1 (ms)	968±106	993±99	972 ± 80	941 ± 94
Accel. Rate	1.7 (Parallel)	3.4 ± 0.5 (CS)	3.5 ± 0.3 (CS)	2.3 ± 0.4 (CS)
Navigator Efficiency (%)	-	52 ± 11	51 ± 12	45 ± 15

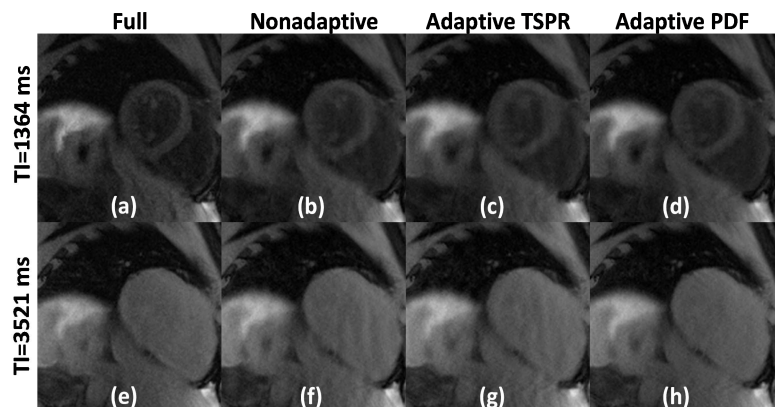


Fig. 2. Comparison of ANGIE images acquired using three different sampling algorithms. **(a,e):** Fully sampled images. Images reconstructed from data with: nonadaptive sampling **(b,f)**, TSPR-based adaptive sampling **(c, g)**, and PDF-based adaptive sampling **(d,h)**. Images **d** and **h** have reduced aliasing artifacts compared to **b-c** and **f-g**, demonstrating that PDF-based adaptive sampling performs better than nonadaptive and TSPR-based adaptive sampling.